Anal. Chem. **2000,** *72,* 376−383

Electrospray Ionization Tandem Mass Spectrometry for Structural Elucidation of Protonated Brevetoxins in Red Tide Algae

Yousheng Hua and Richard B. Cole*

Department of Chemistry, University of New Orleans, Lakefront, New Orleans, Louisiana 70148

Brevetoxins, the toxic components of "red tide" algae, all share one of two robust polycyclic ether backbone structures, but they are distinguished by differing side-chain substituents. Electrospray ionization mass spectrometry analyses of brevetoxins have shown that the polyether structure invariably has a very high affinity for sodium cations that results in the production of abundant $(M + Na)^+$ ions even when sodium cations are only present as impurities. Because the ionic charge tends to remain localized on the sodium atom and because at least two bonds must be broken in order to produce polycyclic backbone fragmentation, it is extremely difficult to obtain abundant product ions (other than Na^+) from $(M + Na)^+$ brevetoxin precursor ions in low-energy collision-induced dissociation (CID) MS/MS experiments. This report establishes that acid additives (oxalic acid, trifluoroacetic acid, and particularly hydrochloric acid) in aqueous methanol solutions can promote high yields of protonated brevetoxin molecules (MH^+ ions) for Btx-1, -2, and -9 brevetoxins. Most importantly, unlike their $(M + Na)^+$ counterparts, MH^+ precursor ions offer readily detectable product ions in CID MS/MS experiments, even under low-energy collisions. This direct structural characterization approach has provided decomposition information from brevetoxins that was previously inaccessible, including the identification of diagnostic product ions for "type A" brevetoxins (*m*/*z* 611) and "type B" brevetoxins (*m*/*z* 779, 473, 179) and characteristic ions for Btx-1 (*m*/*z* 221, 139), Btx-2 (*m*/*z* 153), and Btx-9 (*m*/*z* 157, 85). Precursor ion scans and constant neutral loss scans are proposed to enable screening of individual type A or type B brevetoxins present in naturally occurring mixtures.

Brevetoxins produced from marine algal dinoflagellates *Ptychodiscus brevis* are lipid-soluble polyether neurotoxins that are responsible for massive fish kills and severe human health problems.[1−3] A variety of brevetoxin compounds have been structurally identified and classified as either type A or type B (see Figure 1), with Btx-1 (type A) exhibiting the highest toxicity, and more subtle toxicity differences existing for the individual type B brevetoxins.[4,5] Recently, certain brevetoxin analogues found in shellfish that feed off of dinoflagellates have been structurally identified.[6−8] Other less common brevetoxin components have not been structurally elucidated.[9,10]

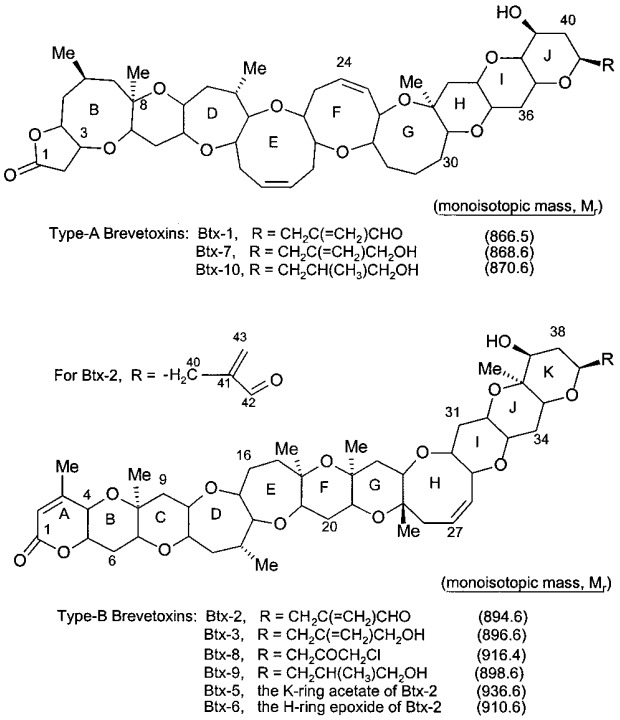

Figure 1. Structures of two main types of brevetoxins.

The mechanism of brevetoxin toxicity has been linked to an alteration of the sodium channel function due to a high degree of

(1) Shimizu, Y. In *Marine Natural Products;* Scheuer, P. J., Ed.; Academic Press: New York, 1978; Vol. I, Chapter 1, pp 1−42.
(2) Music, S. I.; Howell, J. T.; Brumback, C. L. *J. Fla. Med. Assoc.* **1973**, *60*, 27−29.
(3) Pierce, R. H.; Henry, M. S.; Proffitt, L. S.; Hasbrouck, P. A. In *Toxic Marine Phytoplankton*; Granéli, E., Sundström, B., Edler, L., Anderson, D., Eds.; Elsevier Publishing Co.: New York, 1990; pp 397−402.
(4) Rein, K. S.; Lynn, B.; Gawley, R. E.; Baden, D. G. *J. Org. Chem.* **1994**, *59*, 2107−2113.
(5) Baden, D. G.; Mende, T. J.; Szmant, A. M.; Trainer, V. L.; Edwards, R. A.; Rozell, L. E. *Toxicon* **1988**, *26*, 97−103.
(6) Murata, K.; Satake, M.; Naoki, H.; Kaspar, H. F.; Yasumoto, T. *Tetrahedron* **1998**, *54*, 735−742.
(7) Ishida, H.; Nozawa, A.; Totoribe, K.; Muramatsu, N.; Nukaya, H.; Tsuji, K.; Yamaguchi, K.; Yasumoto, T.; Kaspar, H.; Berkett, N.; Kosuge, T. *Tetrahedron Lett.* **1995**, *36*, 725−728.
(8) Morohashi, A.; Satake, M.; Murata, K.; Naoki, H.; Kaspar, H. F.; Yasumoto, T. *Tetrahedron Lett.* **1995**, *36*, 8995−8998.
(9) Hua, Y.; Lu, W.; Henry, M. S.; Pierce, R. H.; Cole, R. B. *J. Chromatogr., A* **1996**, *750*, 115−125.

10.1021/ac990433o CCC: $19.00
Published on Web 12/08/1999

brevetoxin binding to a specific protein site in the sodium channel of mammalian nerve cells.[11−14] In recent years, brevetoxin-related studies have been ongoing in the biological and medical fields. Moreover, brevetoxins have found significant value as neurological probes for investigations of the structure and function of the sodium channel of nerve cells.[15−19] The basic biological processes of ingestion, distribution, and elimination of brevetoxin compounds and their metabolites have also been investigated widely.[10,20−22] Poli et al.[10] did in vitro and in vivo studies of Btx-3 distribution and metabolic fate using rats. They reported three metabolites that are more polar than Btx-3, but they did not identify the structures of these metabolites.

A major challenge is to detect and structurally identify specific brevetoxin metabolites that exist in a complex biological matrix when sample sizes are limited and concentrations are at trace levels. Moreover, certain metabolites are likely to be of limited stability. Many spectrometric methods have been employed to obtain structural information concerning brevetoxins, such as X-ray, NMR, exciton coupled circular dichroism (CD), FT-IR, and UV, as well as a variety of mass spectrometry methods. FT-IR and UV methods serve to assist in confirming the presence of specific functional groups,[23,24] while CD[25] provides conformation information. X-ray[23,24] is a key tool to solving complete chemical structures, but its applications are limited to cases where pure compound crystals are available. NMR spectra in conjunction with electron ionization (EI)-MS data have been used to deduce brevetoxin structures,[26] but NMR also requires relatively large quantities of pure compound, while EI-MS necessitates time-consuming derivatization procedures to convert hydroxyl and lactone functional groups to methoxyl groups. Without derivatization, primarily fragment ions have been observed in EI mass spectra of Btx-1, Btx-3,[27] and Btx-1, Btx-2, and Btx-4.[28] Certain brevetoxins, especially those analogues bearing a carboxylic acid group on the tail side, have been shown to yield abundant $[M - H]^-$ ions by fast-atom bombardment MS.[6,8] Signals were of adequate strength to allow acquisition of tandem mass spectra employing high-energy collision-induced dissociation (CID) on a magnetic sector instrument. $[M - H]^-$ ions exhibited almost exclusively charge-remote fragmentations with negative charge retention on the carboxylate moiety of generated product ions.[6,8]

We have previously established on-line liquid chromatography (LC)/electrospray ionization (ESI)-mass spectrometry as a powerful analytical tool to provide relatively rapid quantitative and structural information concerning brevetoxins with high sensitivity and low sample quantity requirements.[29] But when a single-stage mass spectrometer without tandem mass spectrometry capability is employed, structural information is mainly limited to molecular weight assignments from ionic forms of intact molecules (either singly or multiply charged via cation attachment) and analyte cluster ions (e.g., noncovalently bound dimers and trimers). A good candidate method for profiling the variety of brevetoxin compounds present in a red tide bloom or an ingesting organism, including direct structural elucidation of compounds and metabolites from limited sample quantities, is liquid chromatography coupled to ESI-tandem mass spectrometry (MS/MS).

The strength of the polyether backbone, however, has two major implications for ESI-MS/MS analyses. First, the polyether structure invariably has a very high affinity for sodium cations that results in the initial generation of abundant $(M + Na)^+$ ions even when sodium cations are only present as ubiquitous contaminants in the environment. Second, when attempting to produce collision-induced dissociations, at least two bonds of the polycyclic backbone must be broken in order to obtain backbone fragmentations. This characteristic, combined with the fact that the ionic charge tends to remain localized on the sodium atom, renders it extremely difficult to obtain useful product ions in detectable abundances from brevetoxin $(M + Na)^+$ precursor ions during tandem mass spectrometry experiments. Most frequently, only the uninformative Na^+ product ion is observed in high yield, even under high collision energies obtainable on a magnetic sector instrument. In this paper, we present an alternative method that can be used to obtain ESI-MS/MS spectra whereby protonated molecules MH^+ created under specific solution conditions can decompose under low-energy collision conditions to produce structurally informative product ions. This approach offers potential for future coupling to HPLC for characterization of brevetoxin analogues and their metabolites.

EXPERIMENTAL SECTION

All mass spectrometry experiments were performed on a Quattro II triple-quadrupole mass spectrometer (Micromass Inc., Manchester, England). Sample solutions were directly infused at 2 μL/min into the ESI source employing nitrogen as both nebulizing gas and drying gas. The ESI needle voltage was set at 3.7 kV with the electrospray chamber held at 70 °C and the "cone" voltage set at 40 V. Collision-induced decomposition MS/MS spectra were acquired at 70 eV collision energy (E_{lab}) using argon as the collision gas at a pressure of 2.0×10^{-4} mbar (gauge external to collision cell). All mass spectra represent the average

(10) Poli, M. A.; Templeton, C. B.; Pace, J. G.; Hines, H. B. In *Marine Toxins*; Hall, S., Strichartz, G., Eds.; ACS Symposium Series 418; American Chemical Society: Washington, DC, 1990; pp 176−191.
(11) Poli, M. *J. Assoc. Off. Anal. Chem.* **1988**, *71*, 1000−1002.
(12) Catterall, W. A.; Gainer, M. *Toxicon* **1985**, *23*, 497−504.
(13) Baden, D. G. *FASEB J.* **1989**, *3*, 1807−1817.
(14) Strichartz, G.; Castle, N. In *Marine Toxins*; Hall, S., Strichartz, G., Eds.; ACS Symposium Series 418; American Chemical Society: Washington, DC, 1990; pp 1−20
(15) Trainer, V. L.; Baden, D. G.; Catterall, W. A. *J. Biol. Chem.* **1994**, *269*, 19904−19909.
(16) Nicholson, R. A.; Kumi, C. O. *Pestic. Biochem. Physiol.* **1991**, *40*, 86−97.
(17) Meunier, F. A.; Colasante, C.; Molgo, J. *Neuroscience* **1997**, *78*, 883−893.
(18) Yamamoto, R.; Yanagita, T.; Kobayashi, H.; Yokoo, H.; Wada, A. *J. Neurochem.* **1997**, *68*, 1655−1662.
(19) Cestele, S.; Gordon, D. *J. Neurochem.* **1998**, *70*, 1217−1226.
(20) Rodriguez, F. A.; Maldonado, C. *Puerto Rico Health Sci. J.* **1996**, *15*, 261−267.
(21) Washburn, B. S.; Baden, D. G.; Gassman, N. J.; Walsh, P. J. *Toxicon* **1994**, *32*, 799−805.
(22) Cattet, M.; Geraci, J. R. *Toxicon* **1993**, *31*, 1483−1486.
(23) Lin, Y. Y.; Risk, M.; Ray, S. M.; Van Engen, D.; Clardy, J.; Golik, J.; James, J. C.; Nakanishi, K. *J. Am. Chem. Soc.* **1981**, *103*, 6773−6775.
(24) Shimizu, Y.; Chou, H.; Bando, H.; VanDuyne, G.; Clardy, J. C. *J. Am. Soc. Chem.* **1986**, *108*, 514−515.
(25) Matile, S.; Berova, N.; Nakanishi, K.; Fleischhauer, J.; Woody, R. W. *J. Am. Chem. Soc.* **1996**, *118*, 5198−5206.
(26) Pawlak, J.; Tempesta, M. S.; Golik, J.; Zagorski, M. G.; Lee, M. S.; Nakanishi, K.; Iwashita, T.; Gross, M. L.; Tomer, K. B. *J. Am. Soc. Chem.* **1987**, *109*, 1144−1150.
(27) Chou, H.-N.; Shimizu, Y. *Tetrahedron Lett.* **1982**, *23*, 5521−5524.
(28) Whitefleet-Smith, J.; Boyer, G. L.; Schnoes, H. K. *Toxicon* **1986**, *24*, 1075−1090.
(29) Hua, Y.; Lu, W.; Henry, M. S.; Pierce, R. H.; Cole, R. B. *Anal. Chem.* **1995**, *67*, 1815−1823.

Table 1. Measured Proton Concentration, Acid Concentration, and ESI Intensity of $[Btx\text{-}2 + H]^+$ Peaks in Four Selected Acidic Solutions

	acetic acid pK_a 4.74	oxalic acid pK_a 1.27	TFA pK_a 0.52	HCl pK_a −6.3
$[H^+]$ of 0.001 M acid in 1:1 MeOH/H_2O (M)	9.1×10^{-6}	9.7×10^{-4}	9.9×10^{-4}	1.00×10^{-3}
[acid] with 0.001 M H^+ in 1:1 MeOH/H_2O (M)	0.316	1.02×10^{-3}	1.00×10^{-3}	1.00×10^{-3}
$[Btx\text{-}2 + H]^+$ ESI intensity with 10^{-5} M Btx^{-2} and 0.001 M H^+ in 1:1 MeOH/H_2O (arb units)	3.6×10^5	4.6×10^5	4.3×10^5	4.7×10^5
$[H^+]$ of 0.001 M acid in 4:1 MeOH/H_2O (M)	1.5×10^{-6}	5.2×10^{-4}	8.5×10^{-4}	1.0×10^{-3}
$[Btx\text{-}2 + H]^+$ ESI intensity with 10^{-5} M Btx−2 and 0.001 M H^+ in 4:1 MeOH/H_2O (arb units)	1.2×10^4	3.4×10^4	2.2×10^5	5.7×10^5

of 10−20 scans. All reported m/z values were *rounded down* to the nearest integer value; hence, as there are no nitrogen atoms, and all fragments were assigned as even-electron species, they appear at odd mass values. Solution pH values were measured using a Corning 340 pH meter (Corning Inc., Corning, NY). Brevetoxin standards were purchased from Chiral Corp. (Miami, FL; Btx-1) and Sigma (St. Louis, MO; Btx-2 and Btx-9). Stock solutions of the brevetoxin standards of Btx-1, Btx-2, and Btx-9 were prepared by individually dissolving 50−100 μg of the purchased brevetoxins into 0.5 mL of methanol. Sample solutions were obtained via dilution in specified solvent systems just prior to analyses. HPLC-grade methanol and water were purchased from EM Science (Gibbstown, NJ). Due to their extreme toxicity, it is vital to take appropriate safety precautions when handling brevetoxins, including the use of gloves and safety glasses; disposal must be handled via qualified professionals.

RESULTS AND DISCUSSION

Owing to the very high affinity of brevetoxins for sodium cations, ESI mass spectra employing a single-stage mass analyzer exhibit high-intensity signals for sodium adducts of brevetoxins $(M + Na)^+$ from aqueous methanol solutions prepared at near-neutral pH.[29] However, initial attempts to obtain informative collision-induced dissociation MS/MS spectra using a triple quadrupole from $(M + Na)^+$ precursor ions failed in that the only product ion to appear in detectable yields was Na^+. Even when experiments were repeated on a magnetic sector instrument where high-energy decompositions could be induced, other decomposition products were barely detectable. We postulate that the reason for this is that the ionic charge is localized on the sodium atom, and the decomposition pathway of lowest activation energy is the loss of Na^+, which dominates over any other fragmentation pathway.

An alternative MS/MS strategy that we have developed is to turn to decompositions of protonated brevetoxin molecules, MH^+. Such MH^+ ions from brevetoxins have been observed in positive mode chemical ionization (CI),[23] FAB,[4] and ESI mass spectrometry.[30] In the CI mode, MH^+, $(M + NH_4)^+$, and $(M + Na)^+$ ions were all observed in mass spectra, with MH^+ appearing as a predominant peak,[23] while in the FAB mode, only MH^+ was reported.[4] In ESI, acetonitrile/water sample solutions were acidified with 0.1% trifluoroacetic acid, and both MH^+ and $(M + Na)^+$ ions were observed in about a 2:1 abundance ratio of $MH^+/(M + Na)^+$.[30] In our experience, when employing near-neutral pH solutions, protonated molecules are barely detectable because sodium adducts always dominate. Moreover, initial trials using addition of weak acids (e.g., acetic) resulted in low signals for MH^+ that virtually precluded MS/MS experiments on this precursor ion. Our effort then turned to optimizing solution and instrumental conditions for desorption of MH^+.

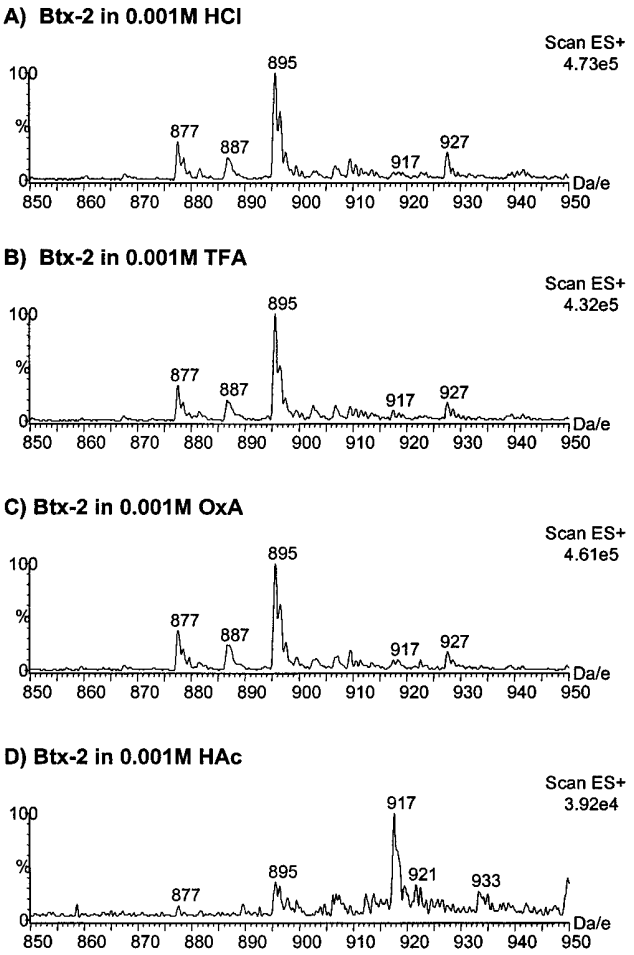

Figure 2. Direct infusion electrospray ionization mass spectra obtained as averages of 10 scans for 1.1×10^{-5} M Btx-2 in 1:1 MeOH/H_2O solutions in varied acid media.

Choice of Acids for Maximizing MH^+ Signal Intensity. Four acids with different dissociation constants (K_a) were selected to test the ability to promote MH^+ formation in ESI mass spectra of Btx-2 (see Table 1). Experiments were conducted either at a fixed concentration of added acid (0.001 M, see Figure 2) or at a fixed (dissociated) proton concentration ($[H^+] = 0.001$ M, Table 1). Proton concentrations (Table 1) were measured with a pH meter that was calibrated using hydrochloric acid solutions in MeOH/

(30) Lewis, R. J.; Holmes, M. J.; Alewood, P. F.; Jones, A. *Nat. Toxins* **1994**, *2*, 56−63.

H_2O (1:1), which were determined (using an approximate pK_a value in MeOH/H_2O (1:1) = 0.5(pK_a (MeOH) + pK_a (H_2O) = −3.0)[31] to completely dissociate under all employed conditions.

When the acid concentration was held constant (0.001 M), but the nature of the added acid was varied (Figure 2), MH^+ abundance for Btx-2 (m/z 895) during ESI-MS increased with rising [H^+] (measured) in the initial solution. From the three acid solutions that underwent virtually complete dissociation (oxalic acid, TFA, HCl), ESI-MS peak intensities were rather similar and of high intensities (full-scale intensity indicated in upper right corner of mass spectrum) relative to pH-neutral solutions. On the other hand, acetic acid addition (relatively high pK_a) offered little improvement in MH^+ signal relative to the pH-neutral solution. In separate experiments, the concentration of acetic acid was increased to 0.316 M, thus raising [H^+] in the initial solution to 0.001 M. Here, MH^+ intensity increased to 3.6×10^5, which is still only ~77% of that of the MH^+ signal obtained from 0.001 M HCl solution (see Figure 2A and Table 1). If one considers the increased level of signal suppression[32−34] due to the very elevated electrolyte concentration in 0.316 M acetic acid, the similar MH^+ intensities under constant [H^+] indicate that a high [H^+] is critical to enabling protonation of brevetoxin molecules. When electrolyte concentration was >0.01 M, signals became severely suppressed.

The above experiment was repeated using the same acid concentration of 0.001 M, but this time a 4:1 methanol/water solution was used as the solvent. As can be seen from the ESI mass spectra (Figure 3), the peak intensity of [Btx-2 + H]$^+$ (m/z 895) decreases monotonically in moving from HCl to HAc solutions, which follows the trend of the relative acidities that decrease in the same direction. The measured proton concentrations for the 0.001 M solutions of the various acids in 4:1 methanol/water are listed in Table 1. Hydrochloric acid solution in 4:1 methanol/water produced the highest intensity protonated Btx-2 peak among the four acids, and this mixed solvent of 4:1 methanol/water was found to perform better than the same quantity of acid added to 1:1 methanol/water. The optimum HCl concentration at 4:1 methanol/water that produces the best [Btx-2 + H^+] signal was determined to be ~(1−2) × 10^{-3} M (Figure 4); Cl^- counterions do little to induce deprotonation.[34−36]

Optimization of Instrumental Parameters. In addition to solution conditions, instrumental parameters can also affect the ESI-MS abundances of protonated brevetoxin molecules. Among these parameters, source temperature, capillary voltage, and cone (skimmer) voltage exhibit significant influences. The optimal temperature range is determined to be between 50 and 70 °C. The cone voltage exerts a marked effect on signal intensity as shown in Figure 5. At a low cone voltage (e.g., 20 V, not shown), the electrostatic lensing properties of the cone are not optimized to allow high transmission of intact brevetoxin ions to the detector. When the cone voltage was raised to 40 V, protonated Btx-2 (m/z 895) appeared in very high intensity (Figure 5A). At 70 V cone voltage (Figure 5B), protonated Btx-2 underwent significant "in-

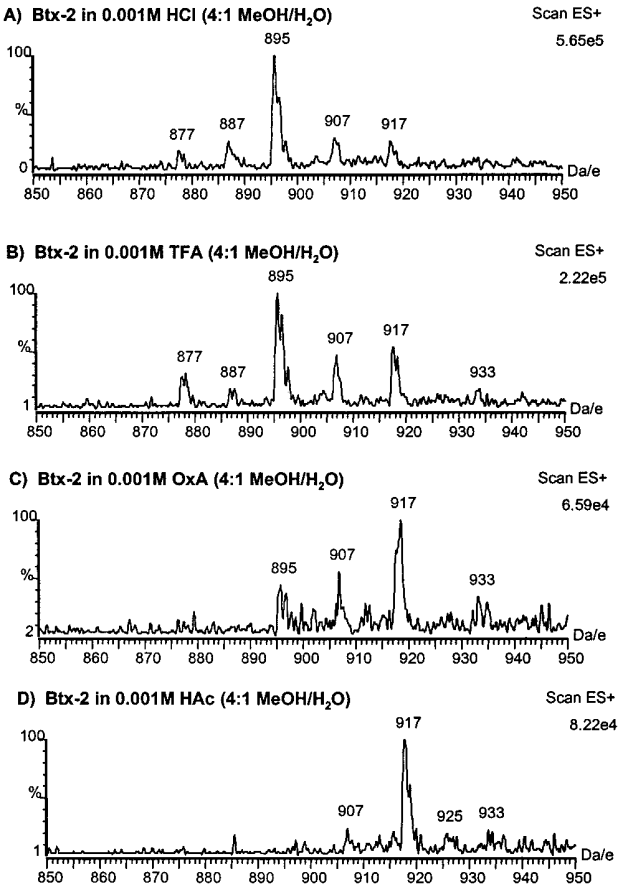

Figure 3. Direct infusion electrospray ionization mass spectra obtained as averages of 10 scans for 1.1×10^{-5} M Btx-2 in 4:1 MeOH/H_2O solutions in varied acid media.

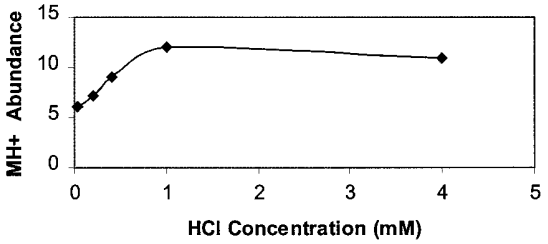

Figure 4. ESI signal intensity of [Btx-2 + H]$^+$ as a function of concentration of hydrochloric acid. Hydrochloric acid was added to Btx-2 solutions to obtain fresh solutions containing 2.1×10^{-5} M Btx-2 in methanol/water (4:1).

source" CID resulting in a reduction in m/z 895 peak intensity, while concurrently the intensity of the peak at m/z 877 (assigned as [Btx-2 + H − H_2O]$^+$) increased. Further increase of the cone voltage to 100 V (Figure 5C) results in continued diminution of m/z 895, while here, m/z 877 decreases in intensity, presumably owing to dominant consecutive decompositions. Last, it is interesting to note that the peak intensity of m/z 917 [Btx-2 + Na]$^+$ actually rises progressively in moving from Figure 5A to Figure 5C. This is indicative of the high stability of sodium adducts of brevetoxins, adducts that are not susceptible to decomposition under in-source CID. The actual increase in the peak intensity of m/z 917 may be attributable to decompositions of noncovalently bound dimers [2Btx-2 + Na]$^+$, doubly charged trimers [3Btx-2 + 2Na]$^{2+}$, and doubly charged dimers [2Btx-2 + 2Na]$^{2+}$. These types

(31) Clare, B. W.; Cook, D.; Ko, E. C. F.; Mac, Y. C.; Parker, A. J. *J. Am. Chem. Soc.* **1966**, *88*, 1911−1916.
(32) Ikonomou, M. G.; Blades, A. T.; Kebarle, P. *Anal. Chem.* **1990**, *62*, 957−967.
(33) Tang, L.; Kebarle, P. *Anal. Chem.* **1991**, *63*, 2709−2715.
(34) Wang, G.; Cole, R. B. *Anal. Chem.* **1994**, *66*, 3702−3708.
(35) Mirza, U. A.; Chait, B. T. *Anal. Chem.* **1994**, *66*, 2898−2904.
(36) Wang, G.; Cole, R. B. *J. Am. Soc. Mass Spectrom.* **1996**, *7*, 1050−1058.

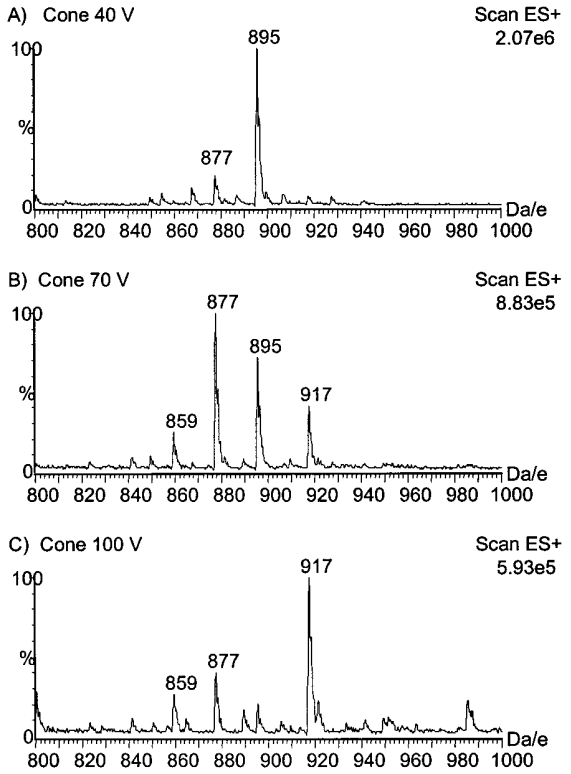

Figure 5. ESI mass spectra of Btx-2 (2×10^{-5} M) in 0.002 M HCl in methanol/water (4:1) solution employing different cone voltages.

of ions were previously observed in ESI mass spectra of brevetoxins.[29]

Tandem Mass Spectra of Brevetoxin Compounds. For the 2.0×10^{-5} M Btx-2 solution in 2.0 mM HCl in 4:1 methanol/water, the $[Btx\text{-}2 + H]^+$ intensity is $\sim 2.1 \times 10^6$ (Figure 5A), which is about 1/5 of the optimized peak height of $[Btx\text{-}2 + Na]^+$ for the same solution devoid of acid. Thus, from the standpoint of quantitation, $[Btx\text{-}2 + Na]^+$ can provide a better signal than $[Btx\text{-}2 + H]^+$. But for tandem mass spectrometry purposes, only $[Btx\text{-}2 + H]^+$ will produce informative fragment ions (Figure 6A).

There are several preferred sites of protonation on the Btx-2 molecule, including the hydroxyl oxygen of the K-ring, the R-group (side-chain) aldehyde oxygen, or any one of several ether oxygens. The proton affinities of hydroxyl oxygens, aldehyde oxygens, and ether oxygens are reported to have rather similar values;[37] hence, a distribution of protonation sites is expected. Moreover, protons can have considerable mobility on the surface of a gas-phase molecule, especially after internal energy is imparted to the protonated molecule upon collision. Comparison of ESI mass spectra of $[Btx\text{-}2 + H]^+$ and $[Btx\text{-}9 + H]^+$ obtained under identical conditions indicates that protonation of Btx-2 is more favorable than protonation of Btx-9. Of course, the structures of Btx-2 and Btx-9 are the same except for the "tail side" (R-group), where Btx-2 has two unsaturations (double bonds) which render the mass of Btx-2 four units lower than that of Btx-9. A major factor contributing to this higher tendency for protonation of Btx-2 is the higher proton affinity[37] of the Btx-2 R-group (810.5 kJ/mol for $CH_2{=}CHCHO$) as compared to that of Btx-9 (792.5 kJ/mol for CH_3-

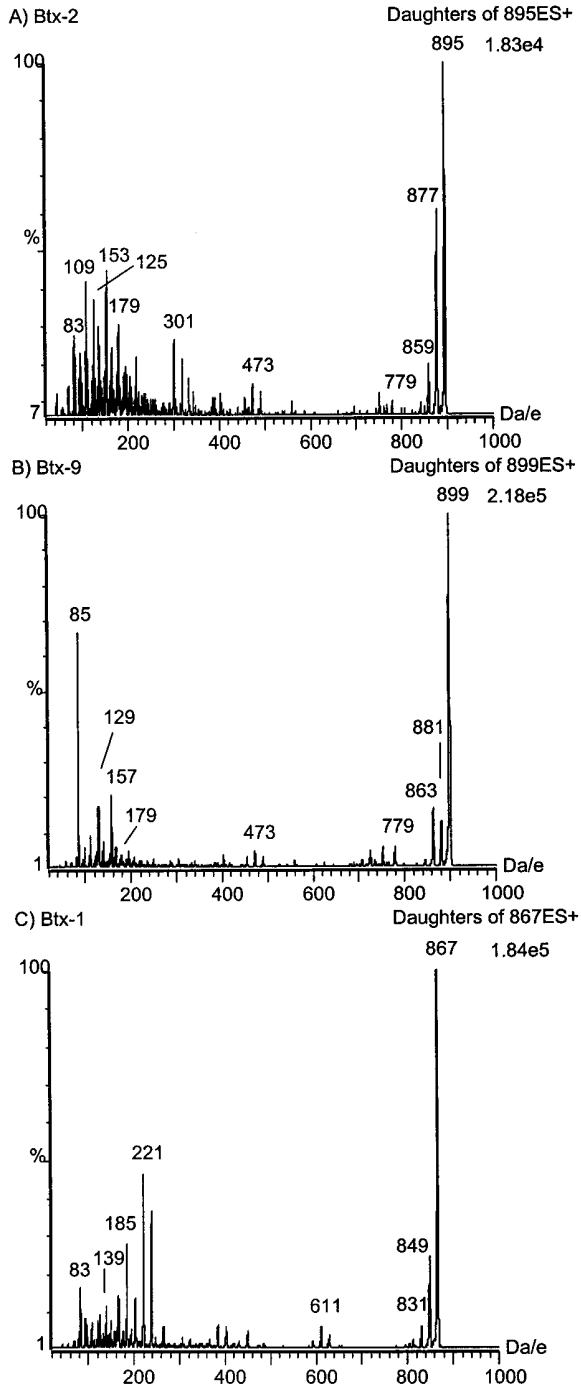

Figure 6. ESI-MS/MS spectra of MH^+ precursor ions (base peaks) of brevetoxins in 0.002 M HCl in methanol/water (4:1) solutions: (A) 2.0×10^{-5} M Btx-2; (B) 1.1×10^{-4} M Btx-9; (C) and 1.1×10^{-4} M Btx-1.

CH_2CH_2OH) located on otherwise identical brevetoxin backbones (see Figure 1).

Panels A–C of Figure 6 show the MS/MS product ion mass spectra of $[Btx\text{-}2 + H]^+$, $[Btx\text{-}9 + H]^+$, and $[Btx\text{-}1 + H]^+$, respectively, obtained under the same instrumental conditions for CID (see Experimental Section). The peaks corresponding to small neutral losses giving product ions at m/z 877, 859, and 841 (Figure 6A) are interpreted to correspond to consecutive water losses involving one, two, and three water molecules. Similar water loss peaks from Btx-9 are found at m/z 881, 863, and 845 (Figure

(37) Lias, S. G.; Bartmess, J. E.; Liebman, J. F.; Holmes, J. L.; Levin, R. D.; Mallard, W. G. *J. Phys. Chem. Ref. Data* **1988**, *17* (Suppl. 1), 117–126.

Scheme 1. Proposed Fragmentation Routes Leading to *m/z* 881, 85, and 779 from [Btx-9 + H]$^+$

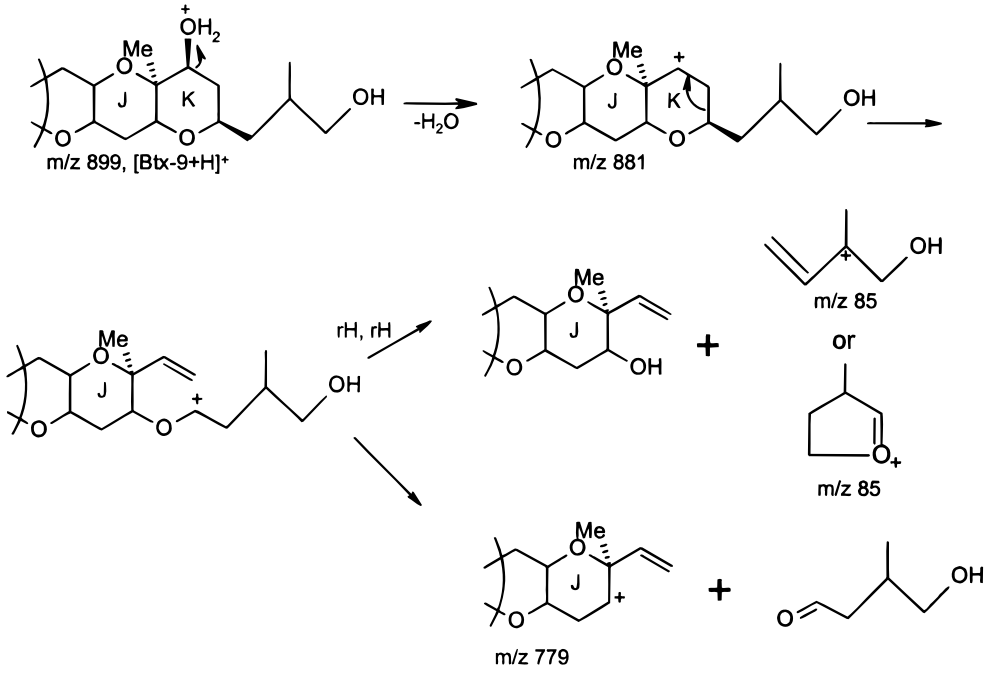

6B). In viewing the lower mass range in Figure 6, there is a major peak at *m*/*z* 85 (highest abundance product ion) that is dominant only in Figure 6B. The *m*/*z* 85 ion is proposed to be formed via dissociation of the "tail end" involving multiple H-transfers to form either of the two stabilized *m*/*z* 85 structures shown in Scheme 1. The MS/MS spectrum of [Btx-9 + H − H_2O]$^+$ (*m*/*z* 881, Figure 7) also gives a dominant peak at *m*/*z* 85, thereby providing additional evidence that the first step in this decomposition is loss of water. An analogous pathway to produce *m*/*z* 81 from [Btx-2 + H]$^+$ is apparently not favorable because of the two additional unsaturations on the tail side that can limit the possibilities for H-transfer from the tail side, yet a moderate intensity peak at *m*/*z* 83 does appear (Figure 6A). Scheme 1 also shows a route to produce a product ion at *m*/*z* 779 from [Btx-9 + H] $^+$ (Figure 6B). This route can also rationalize how [Btx-2 + H]$^+$ produces the same *m*/*z* 779 product ion (Figure 6A). We propose that *m*/*z* 779 represents a diagnostic product ion for the type B brevetoxin backbone structure because it contains 10 intact backbone rings of type B brevetoxin, and it is formed by opening the last (K) ring adjacent to the tail side chain. The side chain, which is what distinguishes the different type B brevetoxins, is lost as a neutral. Our proposed mechanism is corroborated by the appearance of *m*/*z* 779 in the MS/MS product ion spectrum of [Btx-9 + H − H_2O]$^+$ (Figure 7).

Comparison of panels A and B of Figure 6 also reveals that ions at *m*/*z* 473 and 179 appear for both Btx-2 and Btx-9, indicating that in each case charge retention occurs on the head side portions, while the tail-containing portions are lost. A proposed fragmentation mechanism leading to *m*/*z* 473 is shown in Scheme 2 using Btx-2 as an example compound. Here, protonation of an ether oxygen leads directly to ring-opening and a secondary carbocation intermediate. The key structural feature involved in this mechanism is shown for the general case in Figure 8a. For Btx-2 or Btx-9, a mechanism entirely analogous to that shown in

Scheme 2. Proposed Fragmentation Route to *m/z* 473 after Initial Protonation on the Ether Oxygen of Btx-2

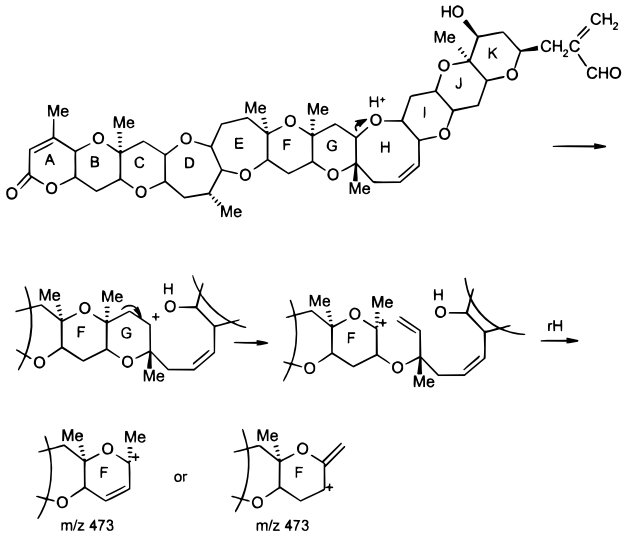

Scheme 2, can occur to form *m*/*z* 179 (proposed structures shown in Figure 8b), based on an initial protonation at the D-ring oxygen. Moreover, an analogous structural portion is also found in the Btx-1 molecule, and indeed a corresponding peak appears at *m*/*z* 611 (Figure 6c, proposed structures shown in Figure 8c). Again, a mechanism analogous to that shown in Scheme 2 can lead to formation of *m*/*z* 611 based upon initial protonation of the I-ring oxygen of Btx-1.

This proposed mechanism, involving initial ether oxygen protonation, is corroborated by the MS/MS product ion spectrum of [Btx-9 + H − H_2O]$^+$ (*m*/*z* 881). These *m*/*z* 881 ions had most likely undergone single water loss after initial protonation of a hydroxyl group on Btx-9, and they did not produce peaks above

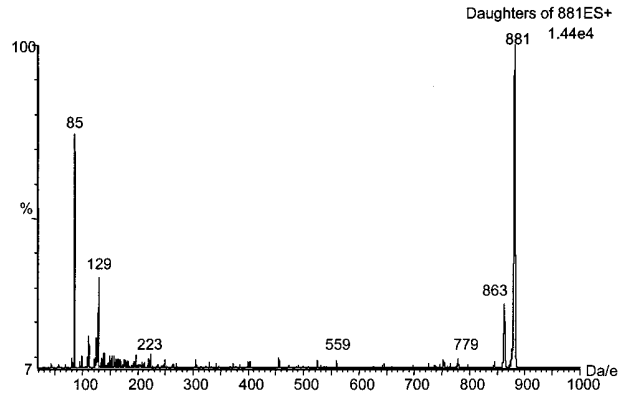

Figure 7. ESI-MS/MS spectrum of $[Btx\text{-}9 + H - H_2O]^+$ (*m*/*z* 881) precursors formed by in-source CID of $[Btx\text{-}9 + H]^+$ precursors.

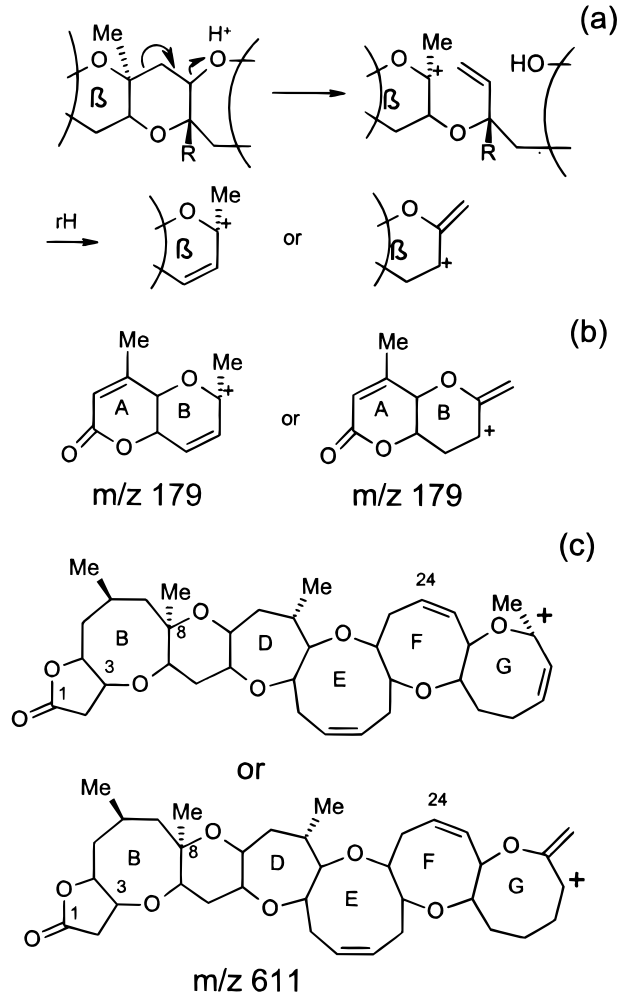

Figure 8. (a) General structural feature and mechanism that leads to ions of (b) *m*/*z* 179 from Btx-2 and Btx-9 and (c) *m*/*z* 611 from Btx-1.

the noise level at *m*/*z* 473 or 179 (Figure 7). This finding suggests that initial protonation on the ring hydroxyl oxygen disfavors the formation of *m*/*z* 179 and 473 ions and adds credibility to the mechanism detailed in Scheme 2 (general case, Figure 8a) depicting initial protonation of an ether oxygen. On the basis of the above arguments, *m*/*z* 473 and 179 (Figure 6A and B) can be considered to be diagnostic ions of the type B brevetoxin backbone structure. Similarly, *m*/*z* 611 (appearing in moderate intensity around the middle-mass range, Figure 6C) can be considered as a diagnostic ion for the type A brevetoxin backbone.

Many peaks appear in the low-mass range for all investigated brevetoxin compounds. Several peaks in Figure 6B (*m*/*z* 129, 139, and 157) are exactly 4 mass units higher than corresponding peaks in Figure 6A (*m*/*z* 125, 135, and 153). These peaks are likely fragmentation ions incorporating and exhibiting charge retention on the "tail" side R-group, because the tail of Btx-9 is exactly 4 mass units heavier than that of Btx-2. Moreover, because of the fact that the "tails" of Btx-2 and Btx-1 are identical, several low-mass ions in Figure 6C from Btx-1 (*m*/*z* 81, 83, 95, 109, and 125) also appear in Figure 6A from Btx-2. Presumably these ions are formed with charge retention on the tail portion.

Scheme 3 has been constructed to rationalize the tail side fragmentation pathways. The diagram starts with protonation on the J-ring hydroxyl group, followed by water loss. The charge migrates from C_{39} to C_{37} upon inductive bond cleavage between C_{37} and C_{38}. A hydrogen transfer to the I-ring oxygen can lead to ring opening. From here, two decomposition pathways are proposed: (1) H-ring opening through inductive bond cleavage, followed by carbon−oxygen cleavage to destroy the H-ring and form a product ion of *m*/*z* 221 (Scheme 3, bottom left). This latter ion is stabilized by multiple conjugation; (2) H-transfer from C_{35} position to the J-ring ether oxygen (via five-membered ring), followed by inductive bond cleavage, to form the product ion of *m*/*z* 139 (Scheme 3, bottom right). Pathways completely analogous to this latter route also apply to Btx-2 and Btx-9 to produce ions of *m*/*z* 153 and 157, respectively, upon substitution of the appropriate R_1 and R_2 groups and bearing in mind that initial protonation takes place at the K-ring hydroxyl group. However, the ions analogous to *m*/*z* 221 formed from Btx-1 according to the first decomposition pathway (i.e., *m*/*z* 235 for Btx-2 and *m*/*z* 239 for Btx-9) were not observed. This may be rationalized by considering that the methyl group attached to the G-ring of Btx-1 effectively stabilizes the charge on C_{32} upon H-ring opening (Scheme 3). However, no analogous methyl group exists on C_{30} (between the H-ring and the I-ring on type B compounds) to stabilize either Btx-2 or Btx-9; hence, the pathway is disfavored.

The peaks corresponding to all four ions depicted in Scheme 3 appear in relatively high intensities in Figure 6. Most importantly, they are all deduced to represent ions that contain the initial side chains that distinguish the various brevetoxins. Because the side chains that differentiate the individual brevetoxins retain the charge, we propose that the associated lost neutrals can be used in diagnostic constant neutral loss MS/MS scans to screen for type A or type B brevetoxins contained in naturally occurring brevetoxin mixtures. The neutral losses of 646 and 728 m_r (leading to product ions of *m*/*z* 221 and 139, respectively, characteristic of Btx-1) are proposed to be diagnostic of type A brevetoxins, while the neutral loss of 742 m_r (associated with the formation of *m*/*z* 153 (Btx-2) and 157 (Btx-9)) is proposed to be diagnostic of type B brevetoxins.

CONCLUSION

Optimization of acidic solution conditions has promoted the desorption of protonated brevetoxin molecules, despite the high affinity of brevetoxins for ubiquitous sodium cations. ESI-MS/MS of MH^+ ions allows efficient decompositions of the polycyclic

Scheme 3. Multistep Fragmentation of [Btx-1 + H]$^+$, Initially Protonated on the J-Ring Hydroxyl Group

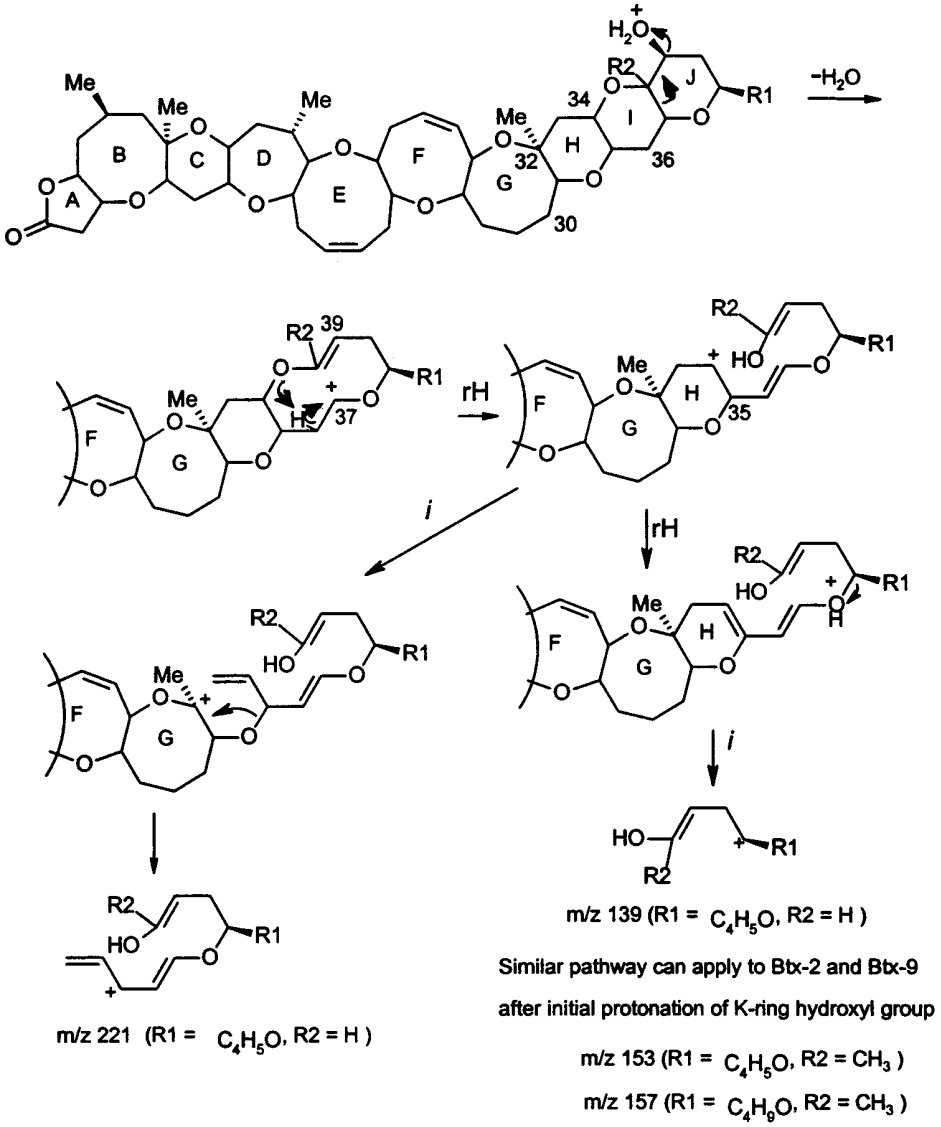

brevetoxin backbone leading to abundant production of structurally informative product ions. This situation is in marked contrast to $(M + Na)^+$ precursor ions that do not produce abundant yields of brevetoxin product ions. Hydrochloric acid in 4:1 methanol/water solution afforded the highest intensity MH^+ signal among four tested acid solutions. The optimum conditions for protonation will depend, of course, on traits of the analyte (e.g., basicity), other solution characteristics, and instrumental parameters. Three fragmentation schemes have been given to rationalize MS/MS decompositions of brevetoxin compounds. Product ion spectra reveal fragments composed of either brevetoxin side-chain and/or backbone structures. Product ions of m/z 779, 473, and 179 can be considered to be diagnostic ions for the type B brevetoxin backbone structure, while m/z 611 can be considered as a diagnostic ion for the type A brevetoxin backbone. We propose that MS/MS precursor ion scans seeking all parents of m/z 779, 473, or 179 can be used to screen for type B brevetoxins, while a precursor ion scan seeking all parents of m/z 611 can locate the type A brevetoxins. Moreover, constant neutral loss scans of 742 m_r (characteristic loss for type B) or 646 and 728 m_r (characteristic losses for type A) can be used to further screen mixtures for brevetoxin constituents. In future studies, in conjunction with LC or CE, the developed ESI-MS/MS approach will find application to brevetoxin metabolite analyses.

ACKNOWLEDGMENT

The authors gratefully acknowledge the Louisiana Board of Regents Support Fund for financial support of this research through Grant LEQSF(1998-01)-RD-B-17. Mass spectrometry equipment support was provided by the National Science Foundation through Grant CHE-9512155 and by the W. M. Keck Foundation. We thank Professor Jean-Claude Tabet for helpful discussions concerning the structure of m/z 85 in Scheme 1.

Received for review April 23, 1999. Accepted October 27, 1999.

AC990433O